MOLECULAR GENETICS

10.1126/sciadv.1600963

POLRMT regulates the switch between replication primer formation and gene expression of mammalian mtDNA

Inge Kühl,[1] Maria Miranda,[1] Viktor Posse,[2] Dusanka Milenkovic,[1] Arnaud Mourier,[1,3] Stefan J. Siira,[4] Nina A. Bonekamp,[1] Ulla Neumann,[5] Aleksandra Filipovska,[4] Paola Loguercio Polosa,[6] Claes M. Gustafsson,[2] Nils-Göran Larsson[1,7]*

Mitochondria are vital in providing cellular energy via their oxidative phosphorylation system, which requires the coordinated expression of genes encoded by both the nuclear and mitochondrial genomes (mtDNA). Transcription of the circular mammalian mtDNA depends on a single mitochondrial RNA polymerase (POLRMT). Although the transcription initiation process is well understood, it is debated whether POLRMT also serves as the primase for the initiation of mtDNA replication. In the nucleus, the RNA polymerases needed for gene expression have no such role. Conditional knockout of *Polrmt* in the heart results in severe mitochondrial dysfunction causing dilated cardiomyopathy in young mice. We further studied the molecular consequences of different expression levels of POLRMT and found that POLRMT is essential for primer synthesis to initiate mtDNA replication in vivo. Furthermore, transcription initiation for primer formation has priority over gene expression. Surprisingly, mitochondrial transcription factor A (TFAM) exists in an mtDNA-free pool in the *Polrmt* knockout mice. TFAM levels remain unchanged despite strong mtDNA depletion, and TFAM is thus protected from degradation of the AAA$^+$ Lon protease in the absence of POLRMT. Last, we report that mitochondrial transcription elongation factor may compensate for a partial depletion of POLRMT in heterozygous *Polrmt* knockout mice, indicating a direct regulatory role of this factor in transcription. In conclusion, we present in vivo evidence that POLRMT has a key regulatory role in the replication of mammalian mtDNA and is part of a transcriptional mechanism that provides a switch between primer formation for mtDNA replication and mitochondrial gene expression.

INTRODUCTION

Mitochondria are essential for a variety of metabolic processes, including oxidative phosphorylation (OXPHOS), whereby energy is harvested from food nutrients to synthesize adenosine 5′-triphosphate (ATP). Mitochondrial dysfunction is associated with a number of genetic diseases and is heavily implicated in age-associated diseases, as well as in the aging process itself (*1*, *2*). The regulation of mitochondrial function is complex because the biogenesis of the OXPHOS system is under dual genetic control and requires the concerted expression of both nuclear and mitochondrial genes (mtDNA) (*3*). Mammalian cells contain thousands of copies of a compact double-stranded circular DNA molecule of ~16.6 kb, and the two strands of mtDNA can be separated on denaturing cesium chloride gradients to a heavy (H) and light (L) strand. The mtDNA encodes 13 essential subunits of the OXPHOS complexes, 2 ribosomal RNAs (mt-rRNAs), and 22 transfer RNAs (mt-tRNAs) (*3*–*5*). The intron-free mammalian mtDNA contains one longer noncoding region of ~1 kb, where the H-strand origin of replication (O_H), as well as the promoters for transcription of the H and L strands (HSP and LSP, respectively), are located (*6*, *7*). Transcription initiated at HSP and LSP yields near genome-size polycistronic mitochondrial transcripts (*8*), which are processed to release the individual mt-mRNA, mt-rRNA, and mt-tRNA molecules (*9*). Transcription from LSP produces the mRNA encoding NADH dehydrogenase subunit 6 (*mt-Nd6*) and 8 mt-tRNAs, whereas the remaining 10 mt-mRNAs (translated to 12 proteins), 14 mt-tRNAs, and 2 mt-rRNAs are produced by transcription from HSP (*3*, *5*). All proteins involved in mammalian mtDNA maintenance and expression are encoded in the nuclear genome, synthesized in the cytosol, and imported into the mitochondrial network. Transcription of the mtDNA is carried out by a single-subunit DNA-dependent RNA polymerase (POLRMT) that is structurally related to bacteriophage T7 RNA polymerase (T7 RNAP) (*10*, *11*). Although the mechanisms of substrate selection and binding as well as catalytic nucleotide incorporation seem to be conserved, the mechanisms of promoter recognition, transcription initiation, transition to elongation, and transcription termination are very different, because POLRMT, in contrast to T7 RNAP, depends on auxiliary factors to perform these processes (*4*–*8*, *11*–*15*). According to in vitro studies, initiation of mitochondrial transcription requires three proteins, namely, POLRMT, the mitochondrial transcription factor B2 (TFB2M), and the mitochondrial transcription factor A (TFAM) (*9*, *10*, *12*). First, sequence-specific binding of TFAM to regions upstream of the transcription start position induces drastic bending of the mtDNA (*4*, *15*–*17*). Second, POLRMT is recruited to HSP and LSP by concerted binding to TFAM and mtDNA sequences in the promoters, as well as sequences upstream of the promoters (*18*, *19*). Formation of this transcription preinitation complex (pre-IC) leads to the recruitment of TFB2M to accomplish promoter melting and initiation of mitochondrial RNA synthesis. Once transcription enters

[1]Department of Mitochondrial Biology, Max Planck Institute for Biology of Ageing, 50931 Cologne, Germany. [2]Department of Medical Biochemistry and Cell Biology, Göteborgs Universitet, 40530 Göteborg, Sweden. [3]Université de Bordeaux and the Centre National de la Recherche Scientifique, Institut de Biochimie et Génétique Cellulaires UMR 5095, Saint-Saëns, F-33077 Bordeaux, France. [4]Harry Perkins Institute of Medical Research, Centre for Medical Research and School of Chemistry and Biochemistry, The University of Western Australia, Perth 6009, Australia. [5]Central Microscopy, Max Planck Institute for Plant Breeding Research, 50829 Cologne, Germany. [6]Department of Biosciences, Biotechnologies, and Biopharmaceutics, University of Bari Aldo Moro, 70125 Bari, Italy. [7]Department of Medical Biochemistry and Biophysics, Karolinska Institutet, 17177 Stockholm, Sweden.
*Corresponding author. Email: larsson@age.mpg.de

the elongation step, TFB2M disassociates from the complex (*11*, *13*). The formation of the pre-IC has been suggested to serve as an important point of regulation of transcription in mitochondria (*19*). Several in vitro studies suggest a difference in activity between HSP and LSP, but this question has never been addressed in vivo. In addition to its role in transcription initiation, TFAM is also a DNA packaging factor that coats the entire mtDNA in a sequence-independent manner and wraps it into compacted nucleoid structures (*20*, *21*). TFAM is essential for mtDNA maintenance and is a key factor involved in directly regulating mtDNA copy number in mammals (*22*). Small variations in the TFAM-to-mtDNA ratio can regulate the number of genomes available for mitochondrial gene transcription and mtDNA replication (*23*). TFAM levels and turnover are reported to be regulated by the AAA^+ Lon protease (LONP), which degrades TFAM not bound to mtDNA (*24*, *25*). In vitro studies have suggested that POLRMT plays an essential role in mtDNA replication and acts together with critical nuclear-encoded factors of the mitochondrial replication machinery, that is, mitochondrial DNA polymerase γ (POLγ) (*26*, *27*), the mitochondrial DNA helicase TWINKLE (*28*), and mitochondrial single-stranded DNA binding protein 1 (SSBP1). It is hypothesized that transcription is preterminated in close proximity to the O_H, which is located about 100 base pairs (bp) downstream of LSP. The RNA primer generated in this way is used by the mitochondrial replication machinery to initiate mtDNA replication at O_H (*29*–*34*). However, the in vivo importance of POLRMT in replication primer formation is debated, because the mammalian mitochondrial primase/polymerase (PrimPol) is reported to play a role in mtDNA replication (*35*). Several models have been proposed to explain how mtDNA is primed and replicated (*34*, *36*, *37*). According to the strand displacement model, replication of the H strand is initiated at O_H and continues to displace the parental H strand. The replication machinery reaches the L-strand origin of replication (O_L) after synthesis of two-thirds of the H strand (*38*). When this region of the L strand becomes single-stranded, it forms a stem-loop structure to which POLRMT can bind to produce the RNA primer necessary for initiation of mtDNA replication at O_L (*39*, *40*). Most mammalian mtDNA replication events initiated at the leading strand are abortive and lead to the formation of a triple-stranded structure containing a prematurely terminated nascent H-strand DNA fragment of 650 nucleotides (nt), which is called the displacement (D) loop (*41*). The abortive mtDNA replication product is denoted 7*S* DNA and remains bound to the parental L strand, thereby displacing the H strand. Mitochondrial transcription elongation factor (TEFM) was found to increase the processivity of POLRMT, thus facilitating the synthesis of long polycistronic RNAs (*42*–*44*). Interaction between TEFM and POLRMT was reported to prevent the generation of replication primers and was thus suggested to serve as a molecular switch between replication and transcription (*44*). Further in vivo analysis is required to investigate how such a switch could be regulated in the mitochondria of actively metabolizing cells. The in vivo regulation of coordinated expression and replication of mtDNA still remains one of the most significant gaps in our understanding of mitochondrial function. POLRMT was suggested as a key factor in both of these processes. The role of POLRMT as a primase for mtDNA replication is debated, because nuclear DNA replication is dependent on specific primases distinct from the RNA polymerases needed for transcription of nuclear genes. To address this question, we generated a *Polrmt* knockout mouse model to elucidate the in vivo role of POLRMT in mtDNA replication.

RESULTS

Polrmt is essential for embryo development

We generated a conditional knockout allele for *Polrmt* by targeting exon 3 to disrupt the expression of POLRMT (fig. S1). Germline heterozygous knockout ($Polrmt^{+/-}$) animals were obtained by breeding mice with a heterozygous floxed *Polrmt* allele (+/$Polrmt^{loxP}$) to mice with ubiquitous expression of cre recombinase (+/β-*actin*–*cre*). Subsequent intercrosses of $Polrmt^{+/-}$ mice produced no viable homozygous knockouts (genotyped offspring, n = 56; $Polrmt^{+/-}$, 66%; $Polrmt^{+/+}$, 34%; $Polrmt^{-/-}$, 0%). We therefore proceeded to analyze staged embryos at embryonic day (E) 8.5 (n = 47) and found that 23% of embryos with a mutant appearance all had the genotype $Polrmt^{-/-}$, whereas the normally appearing embryos were either $Polrmt^{+/+}$ (28%) or $Polrmt^{+/-}$ (49%). Loss of POLRMT thus leads to a severely mutant appearance and embryonic lethality at E8.5, similar to the phenotype of other mouse knockouts with germline disruption of genes essential for maintenance or expression of mtDNA (*28*, *45*).

Disruption of *Polrmt* in heart causes dilated cardiomyopathy

To gain further in vivo insights into the role of *Polrmt*, we studied conditional knockout mice (genotype, $Polrmt^{loxP/loxP}$, +/*Ckmm*-*cre*) with disruption of *Polrmt* in heart and skeletal muscle (*46*). Analysis of complementary DNA (cDNA) by reverse transcription polymerase chain reaction (RT-PCR) verified that sequences corresponding to exon 3 of the *Polrmt* mRNA were lacking in the knockout tissues (Fig. 1A). The conditional knockout mice had a drastically shortened life span, and all of them died before 6 weeks of age (Fig. 1B). We found a progressive enlargement of the heart with dilation of the left ventricular chamber without any apparent increase in the left ventricular wall thickness (Fig. 1C). The ratio of heart to body weight progressively increased during the first weeks of postnatal life (Fig. 1D). Electrocardiography (ECG) showed 40% reduction of the heart rate variability, defined as the variation in the time interval between successive heart beats in late-stage conditional knockout mice, whereas the average heart rate was not different from controls (fig. S2).

Loss of POLRMT causes severe mitochondrial dysfunction in heart

Transmission electron microscopy of terminal-stage knockout hearts showed disruption of the tissue organization and abnormally appearing mitochondria with disorganized cristae (Fig. 2A) consistent with mitochondrial dysfunction. Analysis of OXPHOS capacity in *Polrmt* knockout hearts showed that the enzyme activities of complexes I, IV, and V were deficient, whereas the activity of the exclusively nucleus-encoded complex II was normal (Fig. 2B). Consistently, analysis of the levels of assembled OXPHOS complexes by blue native polyacrylamide gel electrophoresis (BN-PAGE) showed reduced levels of complexes I, IV, and V, whereas complex II was unchanged in the *Polrmt* conditional knockout hearts (Fig. 2C). In addition to a reduction of assembled complex V, increased levels of a subcomplex containing the F_1 portion of ATP synthase was found (Fig. 2C). The observed pattern of deficient OXPHOS sparing complex II (Fig. 2B) is typically caused by reduced mtDNA expression. Therefore, we proceeded to analyze mitochondrial transcript levels.

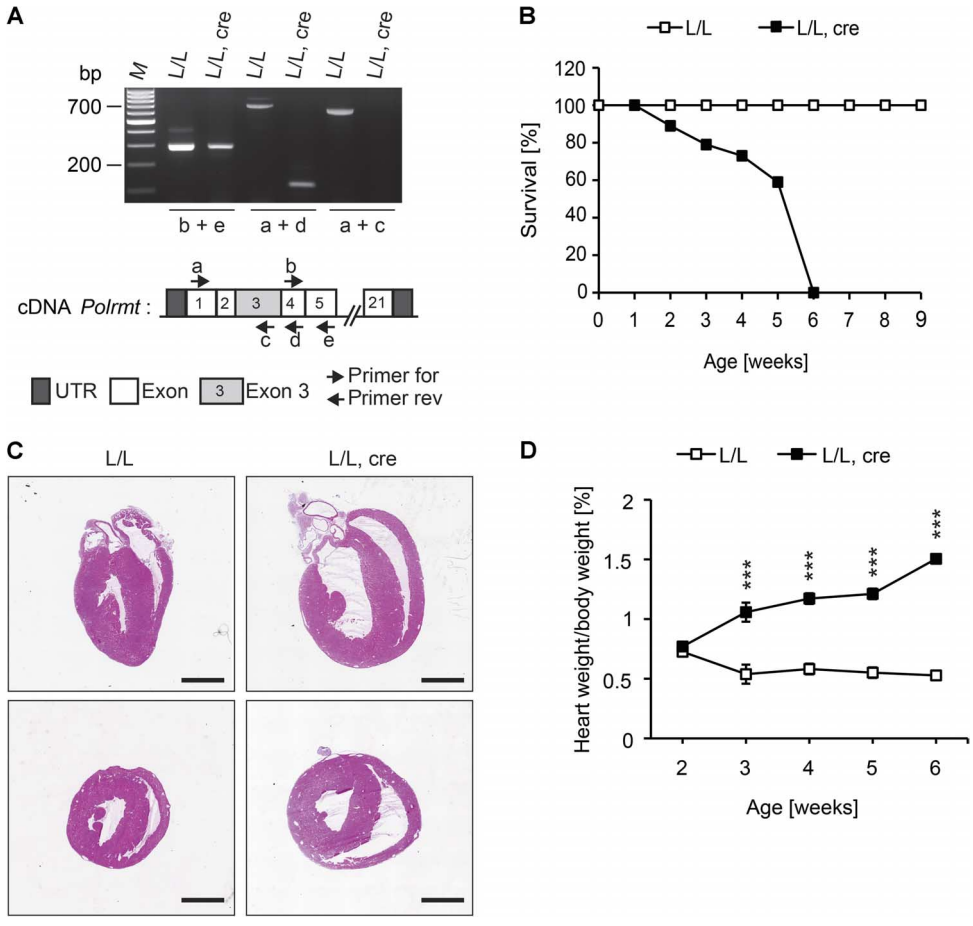

Fig. 1. Knockout of *Polrmt* in germline and heart. (**A**) RT-PCR analysis of *Polrmt* transcripts from control (L/L) and tissue-specific knockout mice (L/L, cre). Different primer sets were used as indicated; exon 3, 551 bp. UTR, untranslated region. (**B**) Survival curve of control ($n = 60$) and tissue-specific knockout ($n = 37$) mice. (**C**) Cardiac phenotype: Vertical (upper panels) and transverse (lower panels) sections through the midportion of hearts of control and tissue-specific knockout mouse hearts at 4 weeks of age. Scale bars, 2 mm. (**D**) Heart–to–body weight ratio of control ($n = 62$) and tissue-specific knockout mice ($n = 57$) at different time points. Error bars indicate ±SEM (***$P < 0.001$; two-tailed Student's t test).

POLRMT synthesizes primers for mtDNA replication initiation

We did not detect the 7*S* RNA transcript in *Polrmt* knockout hearts (Fig. 3A). The 7*S* RNA is the most promoter-proximal transcript formed by transcription initiation at the LSP of mtDNA (*47*). In vitro studies have suggested that transcription from LSP may also form primers for initiation of mtDNA replication. To further elucidate this possibility, we studied levels of D-loop strands referred to as 7*S* DNA (Fig. 3B). The levels of 7*S* DNA were profoundly reduced in relation to total mtDNA levels in *Polrmt* knockout hearts. The steady-state levels of mtDNA were also reduced in hearts lacking POLRMT expression (Fig. 3, C and D). Finally, we determined whether the reduced levels of 7*S* DNA and mtDNA molecules were due to decreased formation or increased degradation by performing in organello mtDNA replication experiments (Fig. 3, E and F). The de novo formation of 7*S* DNA, as well as mtDNA, was much reduced in the absence of POLRMT, consistent with an essential role of this protein in initiation of leading-strand mtDNA replication.

Loss of POLRMT leads to up-regulation of TWINKLE protein levels

To further characterize molecular changes associated with the mtDNA depletion phenotype caused by the absence of POLRMT, we studied the expression of known nuclear-encoded transcription and replication factors, as well as their intramitochondrial interactions. We followed the levels of TFB2M during the progressive depletion of POLRMT in heart and found a parallel decrease in both factors (Fig. 4A and figs. S3, A and B, and S4A), consistent with a previously reported direct molecular interaction between TFB2M and POLRMT (*12*, *19*, *48*). It is important to note that the decrease in TFB2M protein levels occurred despite normal expression of the *Tfb2m* mRNA (Fig. 4B), showing that TFB2M is dependent on POLRMT for its stability. In contrast, TEFM is stable or even slightly increased in the absence of POLRMT (fig. S4, B and C). We further assessed the levels of some important factors involved in mitochondrial RNA metabolism and translation. Both the zinc phosphodiesterase ELAC protein 2 (ELAC2) and the G-rich sequence factor 1 (GRSF1) were strongly increased in *Polrmt* knockout hearts (fig. S4,

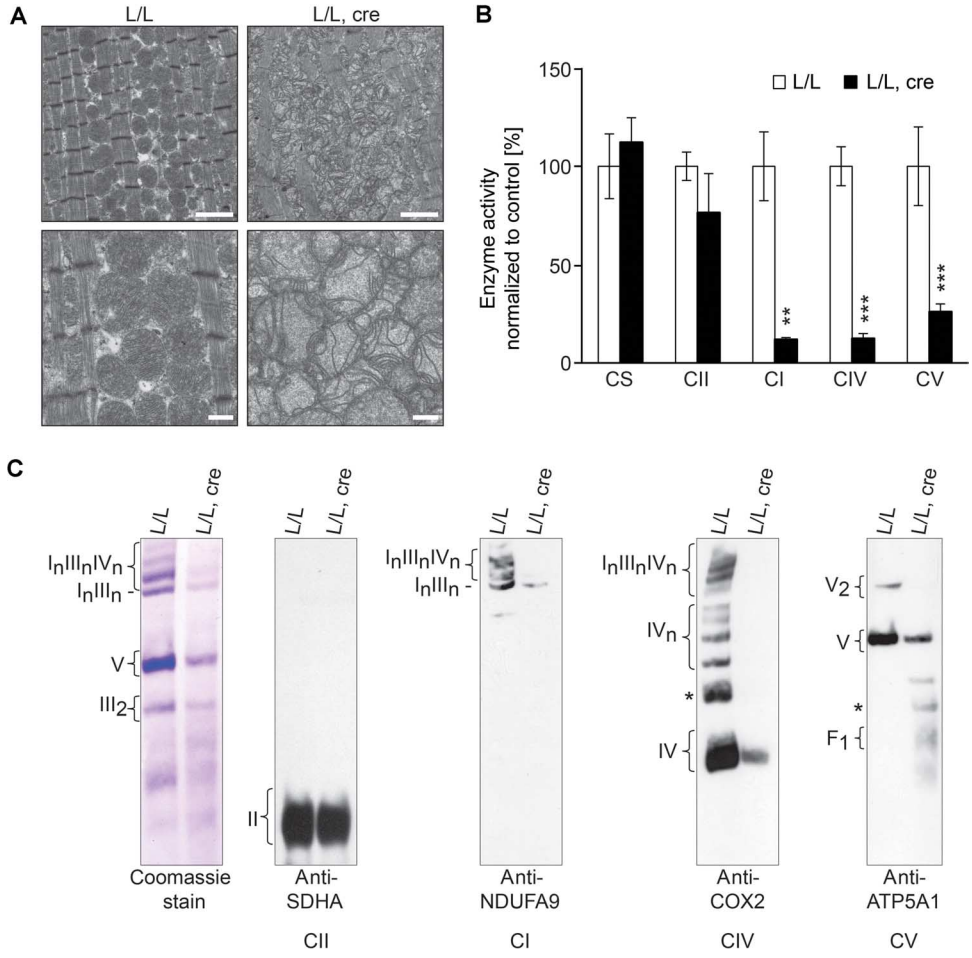

Fig. 2. Reduced OXPHOS capacity in *Polrmt* knockout mouse heart. (**A**) Transmission electron micrographs of myocardium of 5-week-old control ($n = 2$) and tissue-specific knockout mice ($n = 2$). Scale bars, 2 μm (upper panel) and 0.5 μm (lower panel). (**B**) Relative enzyme activities of respiratory chain enzymes measured in mitochondria isolated from hearts of control and tissue-specific knockout mice at different ages. Citrate synthase (CS) was used as an internal control for normalization of the samples. The enzymes measured are citrate synthase; complex II, succinate dehydrogenase; complex I, NADH ubiquinone oxidoreductase; complex IV, cytochrome c oxidase; complex V, adenosine triphosphatase (ATPase) oligomycin-sensitive. All error bars indicate ±SEM (**$P <$ 0.01 and ***$P < 0.001$; $n = 4$; two-tailed Student's t test). (**C**) BN-PAGE analyses of mitochondria isolated from 5-week-old control and tissue-specific knockout hearts. OXPHOS complexes were detected with subunit-specific antibodies or Coomassie Brilliant Blue staining. NDUFA9, complex I; SDHA, 70 kD subunit of complex II; COX2, complex IV; sub α F_1, complex V; respiratory supercomplexes, $I_nIII_nIV_n$ and I_nIII_n.

B and C). ELAC2 is important for RNA processing at the 3′ end of tRNAs (*49*, *50*), and GRSF1 interacts specifically with ribonuclease (RNase) P and is suggested to be involved in early RNA processing events (*51*, *52*). The levels of the leucine-rich pentatricopeptide repeat-containing (LRPPRC) protein (*53*, *54*) were much reduced (Fig. 4A and figs. S3, A and C, and S4A) despite normal levels of *Lrpprc* transcripts (Fig. 4B). Next, we found that the levels of mitochondrial ribosomal proteins of the small and large ribosomal subunits (MRPS35 and MRPL37) were severely reduced in the absence of POLRMT (Fig. 4C and fig. S4, B and C). Noteworthy, the steady-state levels of the 39*S* ribosomal protein L12 (MRPL12), suggested to play a role in regulation of mitochondrial transcription (*55*), were not changed in *Polrmt* knockout hearts (fig. S4, B and C). We found significantly increased protein levels of TWINKLE (Fig. 4A and figs. S3, A and C, and S4A), despite normal levels of *Twinkle* transcripts in *Polrmt* knockout hearts (Fig. 4B), showing that this replicative helicase is stabilized when mtDNA replication is compromised.

An mtDNA-free pool of TFAM appears in absence of POLRMT

Despite severely reduced mtDNA levels, the protein levels of TFAM were unchanged in the absence of POLRMT (Fig. 4A and figs. S3, A and B, and S4A). Furthermore, the steady-state levels of *Tfam* transcripts were increased by ~50% in the knockout hearts, whereas the mRNA expression of the other nucleus-encoded factors was not significantly altered (*Tfb2m*, *Tefm*, *PolγA*, *Ssbp1*, *Mterf2*, *Mterf3*, *Mterf4*, *and Lrpprc*) (Fig. 4B). The AAA^+ LONP, which has been reported to degrade TFAM if not bound to mtDNA (*25*), showed an increased expression (Fig. 4A and figs. S3A and S4A). The finding that TFAM protein levels do not follow the decreased mtDNA levels is very surprising because there are numerous reports of costabilization between TFAM and mtDNA (*56*). We therefore performed linear density glycerol gradient experiments to determine the pools of TFAM that were unbound or present together with mtDNA in the nucleoid (*21*, *57*). The fractions of the gradient containing the nucleoid were determined by the presence

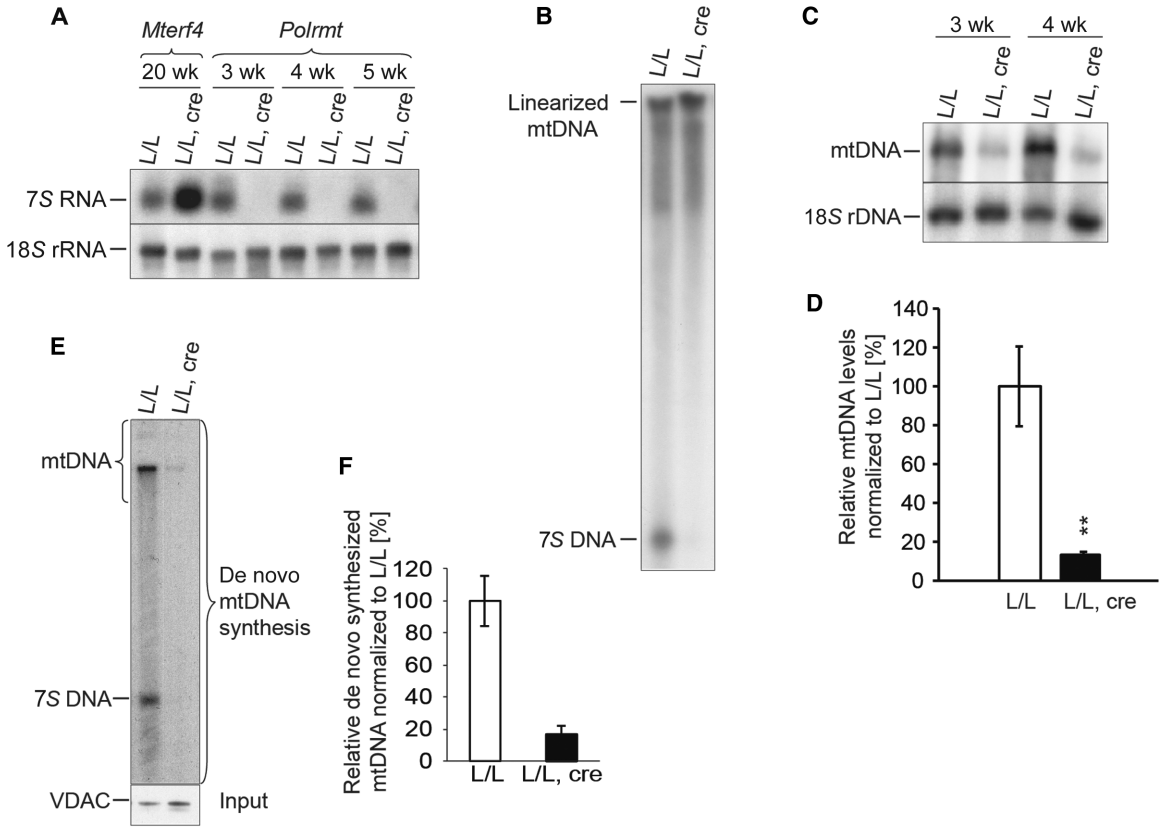

Fig. 3. Decreased mtDNA replication in *Polrmt* knockout mice. (**A**) 7*S* RNA levels in control and tissue-specific knockout hearts at different ages by Northern blot on total RNA; loading, 18*S* rRNA. RNAs from hearts of *Mterf4* conditional knockout mice (*72*) with increased 7*S* RNA levels were loaded as controls. (**B**) Southern blot analyses on mtDNA to assess 7*S* DNA levels of 4-week-old control and tissue-specific knockout mice. To allow relative comparison, the loaded amount of mtDNA from knockouts was higher than the amount loaded from control samples. (**C**) Southern blot analyses on total DNA to assess mtDNA levels of control and tissue-specific knockout mice at different ages; loading, 18*S* rDNA. (**D**) Quantification of Southern blots: mtDNA levels were normalized to 18*S* rDNA and presented as the percentage of controls. Error bars indicate ±SEM (*$P < 0.05$; two-tailed Student's *t* test). (**E**) Levels of de novo–synthesized DNA of isolated heart mitochondria of 4-week-old tissue-specific knockout and control mice. Equal input was ensured by Western blot analysis [voltage-dependent anion channel (VDAC)] on isolated mitochondria after labeling before mtDNA extraction. (**F**) Quantification of the results from (E).

of mtDNA, verified by Southern blotting and deoxyribonuclease (DNase) treatment, and by the presence of replication factors, such as TWINKLE and POLγA (Fig. 4C and fig. S5A). In mitochondria isolated from *Polrmt* knockout hearts, there was a clear increase in TFAM protein levels in the mtDNA-free fractions (Fig. 4, D and E, and fig. S6A). The mtDNA depletion that results from deficient replication primer formation in the absence of POLRMT thus leads to an increased pool of mtDNA-free TFAM that is not degraded despite increased LONP protein levels.

LSP-initiated transcription is favored at low POLRMT levels

Consistent with the previously observed profound reduction in de novo transcription of mtDNA in the absence of POLRMT (*46*), we found a global severe decrease in the steady-state levels of all analyzed mitochondrial mRNAs, rRNAs, and tRNAs (Fig. 5, A to C). Northern blot analysis showed that, in the absence of POLRMT, the levels of several transcripts encoded on the L strand, that is, *mt-Nd6*, *mt-Tp*, *mt-Te*, *mt-Ts2*, *mt-Tc*, *mt-Tn*, and *mt-Tq*, were less decreased than transcripts encoded on the H strand (Fig. 5, A and B). Next, we used RNA sequencing (RNA-Seq) to quantify the reduction in steady-state levels of the mitochondrial transcriptome and found that the *mt-Nd6* transcript showed a much higher relative abundance than mitochondrial rRNAs or the other mt-mRNAs in *Polrmt* knockout hearts from 4-week-old mice (Fig. 5C). To determine whether this difference in mitochondrial transcript steady-state levels was due to promoter-specific transcription initiation effects in heart mitochondria with low POLRMT levels, we performed in vitro transcription assays (Fig. 5, D and E). At low POLRMT concentrations (32 to 0.5 nM), we detected a strong reduction of transcription initiation from HSP in comparison with LSP (Fig. 5, D and E), showing that transcription initiation at LSP is better maintained at low POLRMT levels.

Heterozygous *Polrmt* knockouts increase TEFM levels and maintain transcription

To determine how a moderate reduction of POLRMT levels affects mtDNA expression, we studied *Polrmt*$^{+/-}$ mice. The *Polrmt*$^{+/-}$ mice showed decreased POLRMT protein levels in heart, skeletal muscle, and liver in accordance with a 50% reduction in *Polrmt* gene dosage (Fig. 6A and fig. S7, A and B). A global reduction of POLRMT expression does not cause any phenotype, and the heterozygous knockout

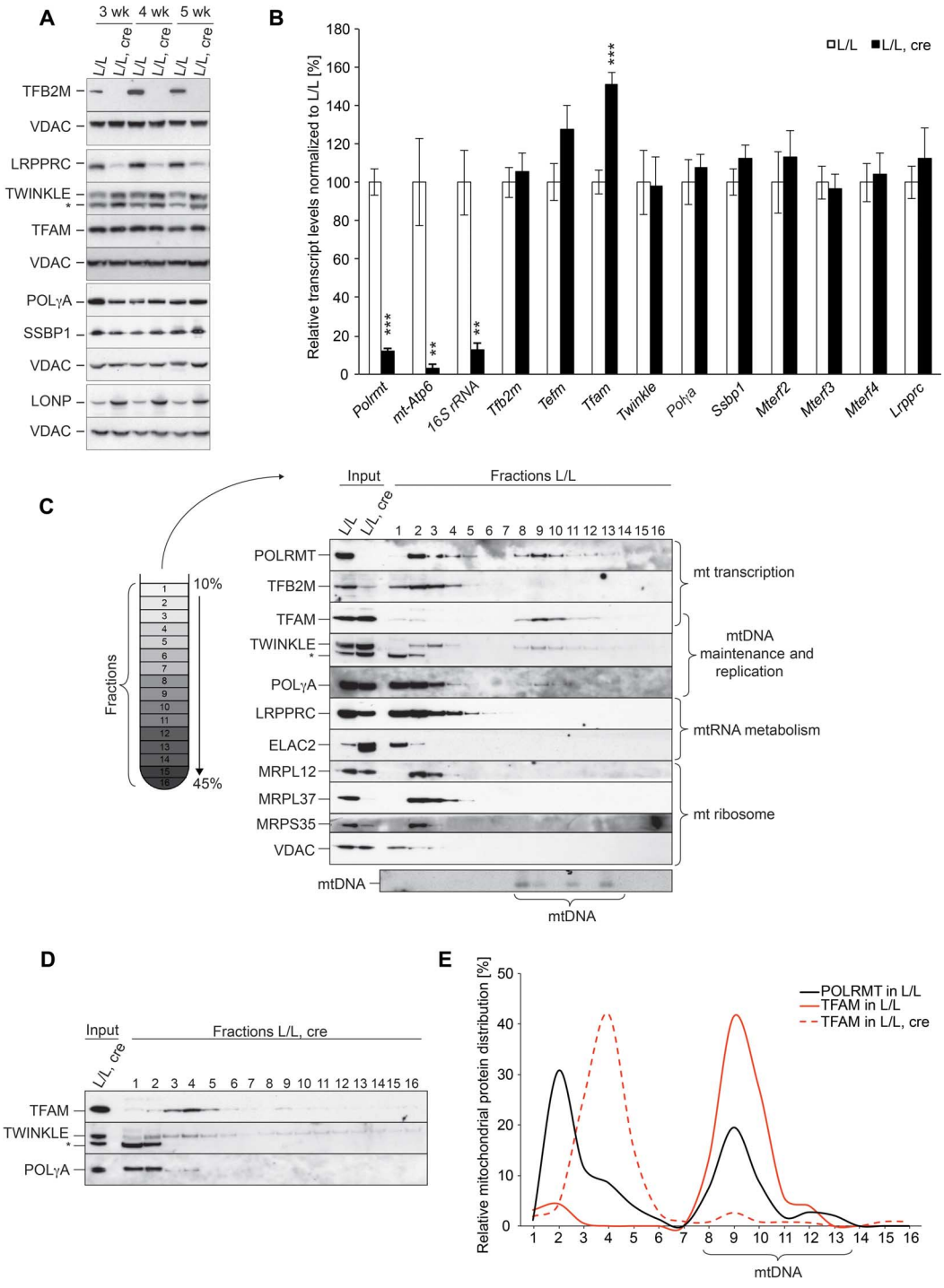

Fig. 4. Loss of POLRMT results in an increased mtDNA-free pool of TFAM. (**A**) Steady-state protein levels of nuclear-encoded factors of mtDNA expression analyzed by Western blotting on mitochondrial extracts from hearts of control and tissue-specific knockout mice; loading, VDAC; asterisk, cross-reacting band (*28*); for quantification, see fig. S4A. (**B**) Quantitative RT-PCR (qRT-PCR) of transcript levels of nuclear-encoded mitochondrial proteins. Normalization, β_2M (β_2-microglobulin). Error bars indicate ±SEM (*$P < 0.05$ and ***$P < 0.001$; two-tailed Student's *t* test; see table S1). (**C** and **D**) Linear glycerol density gradient fractionations of mitochondrial lysates from tissue-specific knockout and control mice followed by Western blot analysis; for quantification, see figs. S5 (A to C) and S6. Samples taken from fractions 1 to 16 are of increasing density (that is, from top to bottom of the tube after separation by ultracentrifugation; as indicated by the schematic representation of the centrifuge tube to the left). Fractions were loaded from left to right on the gels as indicated by the lane numbering; input, aliquots of unfractionated lysates. The mtDNA content of the fractions was determined by Southern blotting. (**E**) Relative TFAM and POLRMT protein distribution across the gradient from control and knockout heart mitochondria.

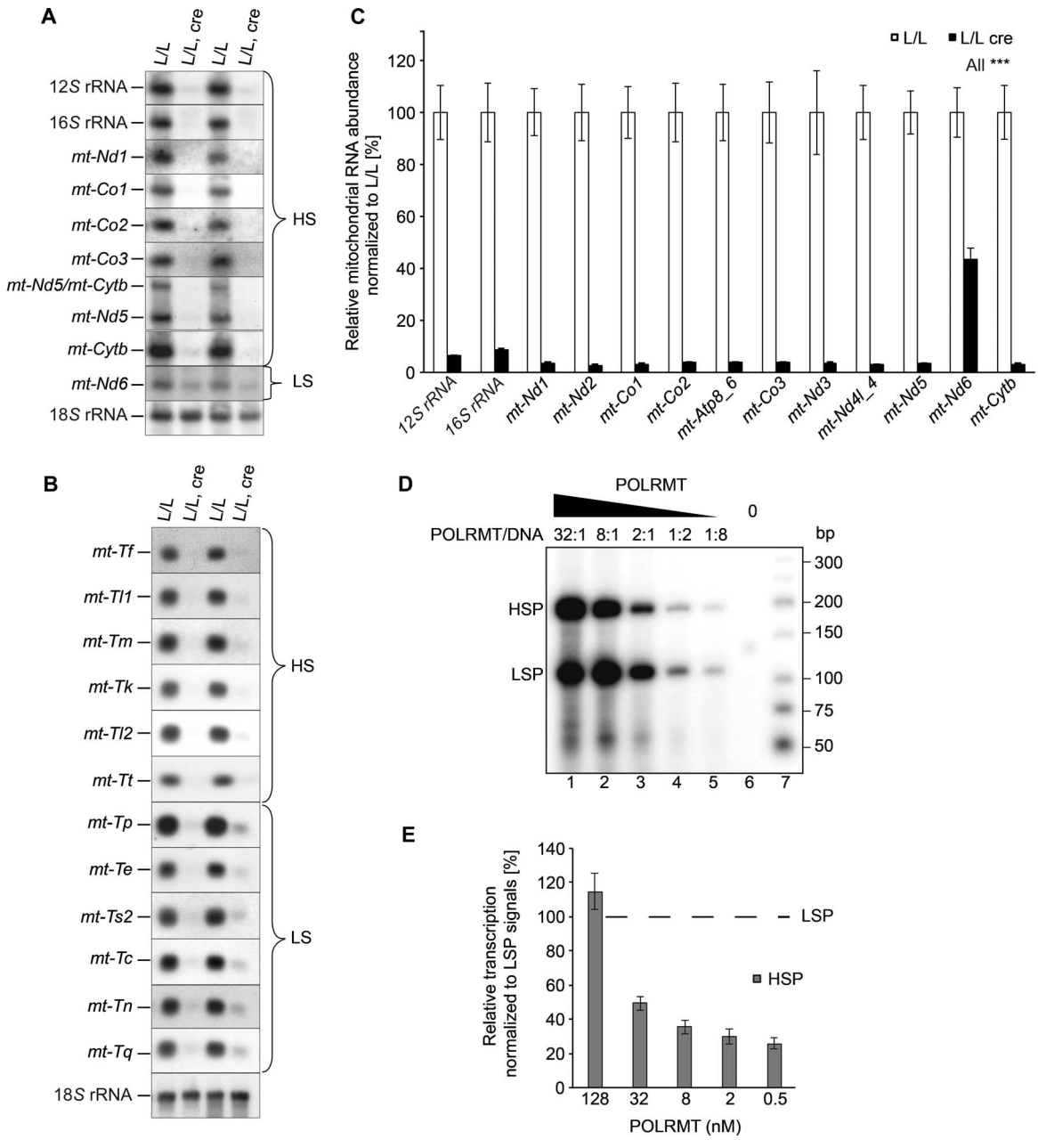

Fig. 5. LSP and HSP show different sensitivities at low POLRMT concentrations. (**A** and **B**) Northern blot analyses of mitochondrial mRNAs, rRNAs, and tRNAs from hearts of 4-week-old control and tissue-specific knockout mice; loading, 18*S* rRNA. (**C**) Relative mitochondrial RNA abundance of mRNA and rRNA levels in hearts of 4-week-old tissue-specific knockout and control mice normalized to the upper quartile of the gene count distribution. The data analyzed are from three independent RNA-Seq experiments; all RNAs have $^{***}P \leq 0.0001$. Error bars indicate ±SEM. (**D**) In vitro transcription assay at different POLRMT levels. All reactions contained a cut plasmid template (containing the human LSP and HSP promoters giving a run-off product of 101 and 180 nt, respectively). POLRMT was added at 128, 32, 8, 2, and 0.5 nM in lanes 1 to 5, respectively; lane 6, control without POLRMT; lane 7, molecular weight marker (New England Biolabs). (**E**) Quantification of the results from (D). The experiment was performed in triplicates, and HSP transcription levels were normalized to LSP for each POLRMT concentration; bars, mean value. Error bars indicate ±SD ($n = 3$).

mice are apparently viable, fertile, and healthy at 1 year of age. We proceeded to determine whether the moderately altered POLRMT levels have an effect on the steady-state levels of OXPHOS enzyme complexes. Western blot analysis of respiratory chain subunits showed normal levels of NDUFB8 (complex I), SDHA (complex II), UQCRC2 (complex III), COX1 and COX2 (complex IV), and ATP5A1 (complex V) in hearts from 26- and 52-week-old *Polrmt*$^{+/-}$ mice (Fig. 6A and fig. S7, C and D). Both Northern blot analysis of steady-state levels of mitochondrial rRNAs, tRNAs, and mRNAs, and RNA-Seq analysis of the mitochondrial transcriptome of *Polrmt*$^{+/-}$ mice in heart showed a normal mitochondrial transcript abundance despite reduced POLRMT levels (Fig. 6B and fig. S8, A and B). Consistent with the normal mt-mRNA levels, the levels of LRPPRC were not changed in *Polrmt*$^{+/-}$ mice (Fig. 6C and fig. S9A). Noteworthy, RNA-Seq data showed that the *mt-Nd6* transcript encoded on the L strand was slightly reduced, whereas all other mitochondrial rRNAs and mRNAs encoded on the H strand showed a tendency to be increased in *Polrmt*$^{+/-}$ hearts at 26 weeks of age (fig. S8B). We observed a strong increase in TEFM protein levels (Fig. 6C and fig. S9A), which may provide a compensatory response to reduced transcription initiation in *Polrmt*$^{+/-}$ mice. This suggestion is supported by the finding of slightly increased de novo transcription in heart mitochondria from *Polrmt*$^{+/-}$ mice (Fig. 6D). Furthermore, the levels of 7*S* RNA are normal in *Polrmt*$^{+/-}$ mice (Fig. 6E), thus showing that promoter proximal transcription at LSP is sufficient

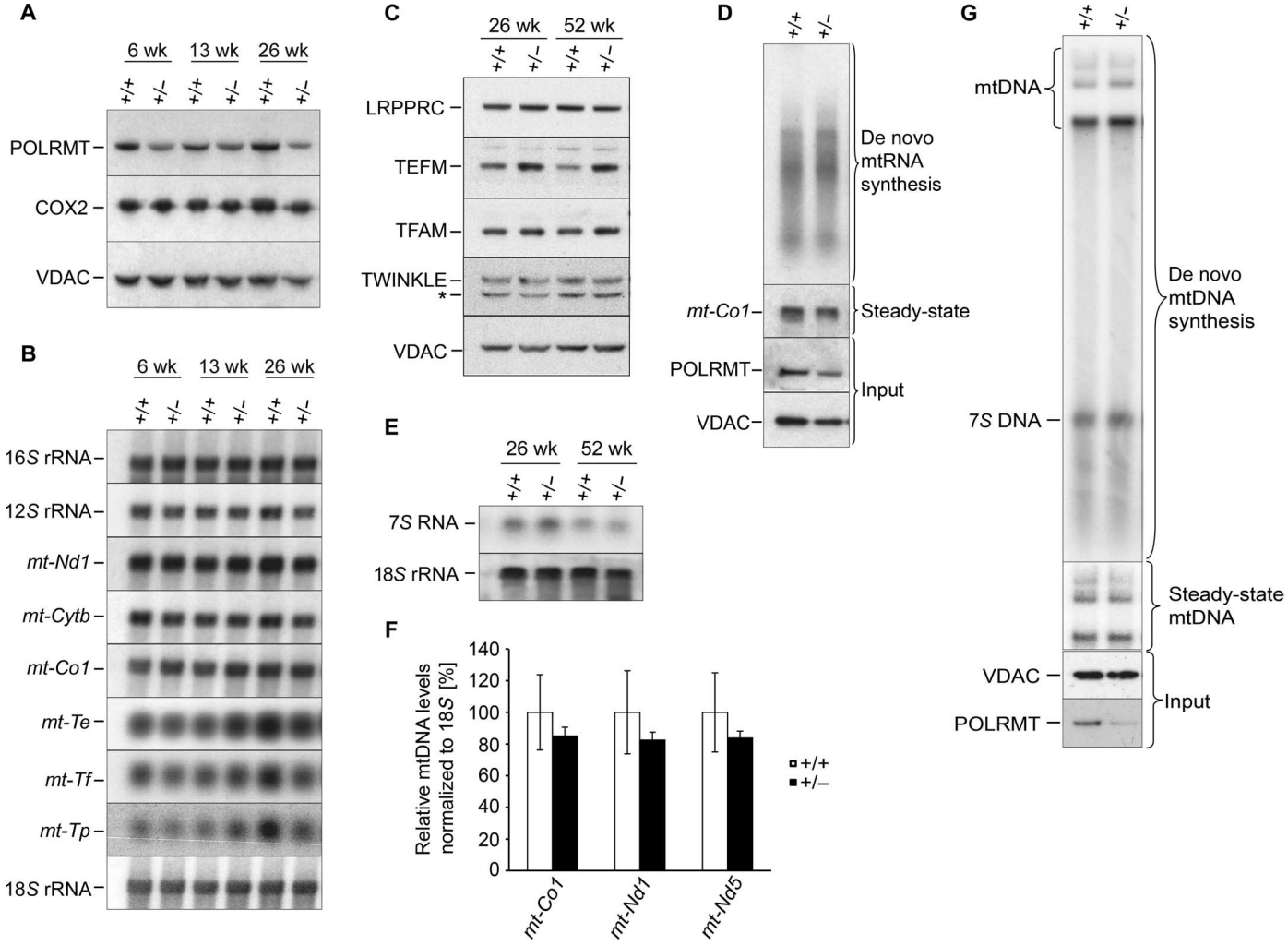

Fig. 6. Characterization of heterozygous *Polrmt* knockout mice. (**A**) POLRMT steady-state protein levels in heart from wild-type (+/+) and heterozygous *Polrmt* knockout (+/–) mice; loading, VDAC; for quantification, see fig. S7C. (**B**) Steady-state levels of mitochondrial mRNAs, rRNAs, and tRNAs; loading, 18*S* rRNA; for quantification, see fig. S8A. (**C**) Steady-state protein levels of nuclear-encoded factors of mtDNA expression analyzed by Western blotting on mitochondrial heart extracts; loading, VDAC; for quantification, see fig. S9A; asterisk, cross-reacting band (*28*). (**D**) De novo–synthesized mitochondrial transcripts from hearts of 52-week-old mice. Steady-state levels of individual mitochondrial transcripts were verified with a radiolabeled probe (*mt-Co1*); input, Western blot analysis (POLRMT and VDAC) after labeling. (**E**) 7*S* RNA levels in mouse hearts by Northern blotting on total RNA; loading, 18*S* rRNA. (**F**) Quantification of mtDNA by quantitative PCR (qPCR) with *mt-Co1*, *mt-Nd1*, and *mt-Nd5* probes on mouse heart. Signals were normalized to the 18*S* signal; $n = 3$. Error bars indicate ±SEM. (**G**) De novo–synthesized DNA of isolated mitochondria from hearts of 12-week-old mice. The mtDNA was radioactively labeled in organello, isolated and boiled to release newly synthesized 7*S* DNA before Southern blotting; input, Western blotting (POLRMT and VDAC) after labeling; for quantification, see fig. S10B.

to maintain mtDNA replication and levels (Fig. 6F and fig. S10A). Consistent with the normal mtDNA levels, the levels of TFAM were not changed in *Polrmt*$^{+/-}$ mice (Fig. 6C and fig. S9A). Also, de novo formation of 7*S* DNA was not decreased when POLRMT was reduced (Fig. 6G and fig. S10B), and the normal levels of TWINKLE, POLγA, and SSBP1 proteins (Fig. 6C and fig. S9, A and B) provide further support for normal mtDNA replication in *Polrmt*$^{+/-}$ mice. Thus, a moderate reduction of POLRMT expression in *Polrmt*$^{+/-}$ mice does not affect overall mtDNA transcription or maintenance.

DISCUSSION

Here, we show that POLRMT, in addition to its essential role in gene expression, is required for primer formation for initiation of mtDNA replication in vivo. Our data show that primer synthesis and initiation of mtDNA replication are prioritized over gene transcription because (i) there is a differential effect of POLRMT at the mtDNA promoters as illustrated in Fig. 7. At lower POLRMT levels, transcription is primarily initiated at LSP, which helps to ensure that primer synthesis can be maintained. (ii) Under normal conditions, about 95% of all replication initiation events at O_H are prematurely terminated, forming the 7*S* DNA. When POLRMT is depleted, 7*S* DNA is no longer formed, suggesting that all residual replicative events continue to full-length replication. (iii) The increase in TWINKLE protein levels is likely a compensatory response aimed to promote productive mtDNA replication. The increased TWINKLE protein levels are most likely due to posttranscriptional regulation because the *Twinkle* mRNA levels remain unchanged. Although the exact mechanisms of TWINKLE stabilization and regulatory role in mtDNA replication remain unknown, TWINKLE can be loaded at the 3′ end of 7*S* DNA to promote full-length genomic replication (*58*). It is possible that abortive mtDNA replication is favored by an antihelicase activity at the end of the D loop (*58*, *59*) and that increased TWINKLE levels will overcome this block. The increase in TWINKLE as a compensatory mechanism agrees with results from other mouse models with severe mtDNA depletion, suggesting an involvement of TWINKLE in the regulation of mtDNA replication in mammals. Surprisingly, the TFAM protein levels remain normal in the absence of POLRMT despite profound mtDNA depletion. The inability of this excess TFAM to bind mtDNA to form nucleoids results in an increased free pool of TFAM. There is strong experimental evidence that the amount of TFAM directly regulates mtDNA copy number and that mtDNA levels also reciprocally affect TFAM levels (*21*, *56*, *60*). Disruption of *Tfam* in mouse leads to loss of mtDNA, and overexpression of *TFAM* leads to increased mtDNA copy number (*22*, *45*). Our data show that TFAM can be stable in the absence of mtDNA. The normal TFAM protein levels observed here could be a part of a compensatory response that attempts to maintain mtDNA. It has been suggested that TFAM turnover involves LONP, which degrades TFAM when it is not bound to mtDNA (*24*, *25*). Overexpression of *LONP* was reported to result in reduced TFAM and mtDNA levels, whereas *LONP* depletion was found to increase TFAM and mtDNA levels. The TFAM protein levels are normal despite increased LONP levels in the absence of POLRMT. TFAM is thus protected from LONP degradation. Moreover, the levels of *Tfam* transcripts were increased in the *Polrmt* knockout hearts, whereas all other investigated transcripts of nuclear genes involved in mtDNA expression were unaltered. These findings argue for a compensatory regulatory

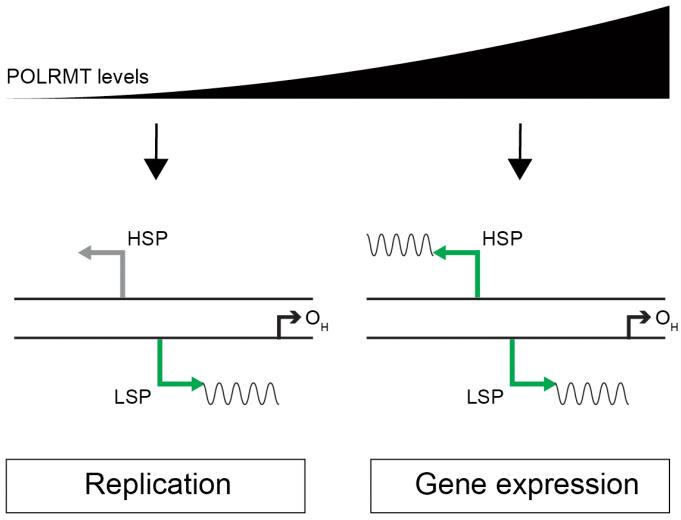

Fig. 7. Model of POLRMT regulating replication primer formation and expression of mtDNA. At high POLRMT levels, mitochondrial transcription initiation is activated from both the HSP and LSP resulting in mtDNA gene expression. At low POLRMT levels, only LSP is active and an RNA primer for replication of mtDNA is synthesized.

mechanism that controls TFAM levels in mitochondria. To our knowledge, this discrepancy between mtDNA and TFAM levels has not been found in other knockout mouse models with reduced mtDNA levels (*28*), and it remains to be clarified whether this is specifically linked to the loss of POLRMT. LONP is known to play a role in degrading misfolded, unassembled, or oxidatively damaged proteins. Thus, the highly induced levels of LONP in the *Polrmt* knockouts are likely due to an imbalance between mtDNA- and nucleus-encoded OXPHOS subunits, as already described in previous studies (*61*). The mechanisms that regulate transcription levels in mammalian mitochondria remain to be clarified, and our study of the heterozygous *Polrmt* knockout mice provides important insights. Despite a drop in POLRMT levels, the steady-state mitochondrial transcript levels in these mice are unchanged. We also observed increased TEFM protein levels, whereas all other nuclear-encoded factors involved in mtDNA expression, for example, LRPPRC, TFAM, and TWINKLE, were normal. This could be a compensatory response to ensure a normal transcription rate and mitochondrial steady-state transcript levels even when the ratio of POLRMT protein per mtDNA molecule is reduced in the heterozygous *Polrmt* knockouts. In vitro studies recently reported that TEFM increases transcription processivity to allow mitochondria to increase transcription rates (*43*, *44*). In contrast to TEFM, neither TFAM nor TFB2M levels were affected in the heterozygous *Polrmt* knockout mice. Both of these factors are directly involved in the transcription initiation mechanism, but apparently, their levels are not limiting in promoting increased levels of transcription. In the nucleus, differential activation of the large number of protein-coding genes is not controlled by varying the amount of RNA polymerase II but is instead based on specific combinations of bound transcription factors that regulate promoter specificity. In contrast to the nucleus, where protein-coding genes typically are present only in two copies per cell, there are thousands of copies of mtDNA per cell. This means that increased transcription of mtDNA does not necessarily require increased transcription from each promoter, but it can instead be achieved by engaging more mtDNA templates in

transcription. This mode of regulation will only be an efficient regulatory system if the number of target promoters is low, such as is the case for mtDNA that only has two promoters per genome. How the presence of TEFM may prevent early transcription termination and promote transcription beyond the immediate promoter region remains to be discovered. The genetic data we present here resolve the controversy concerning the role of POLRMT as a primase for mammalian mtDNA replication. This issue has been widely debated because nuclear DNA replication is dependent on specific primases, which are distinct from the RNA polymerases needed for transcription of nuclear genes. Our mouse knockout data show that in the absence of POLRMT, 7*S* DNA is no longer formed, and there is a severe reduction of mtDNA levels. In vitro data have shown that POLRMT can generate the RNA primers needed for mtDNA synthesis at both O_H and O_L (*40*), but the in vivo importance of these findings has not been established (*62*). The 7*S* RNA, a polyadenylated transcript that is terminated near the 5′ end of the nascent D loop strand, is undetectable in the absence of POLRMT. The function of the 7*S* RNA is not clear, but it has been suggested that it is involved in primer formation for initiation of mtDNA synthesis at O_H (*36*, *58*). In mammalian mitochondria, PrimPol was reported to have DNA and RNA primase activities and play a role in mtDNA replication (*35*). Our knockout data show that PrimPol or any other primase cannot complement for the absence of POLRMT when it comes to mtDNA replication initiation. Together, our study provides clear evidence that POLRMT functions as the primase for mtDNA replication in mammalian mitochondria in vivo. Deletion of *Polrmt* in heart results in a severe decrease in all mitochondrial transcripts, but we also report that the mitochondrial transcripts derived from the L strand, in particular the *mt-Nd6* mRNA, are less reduced than those transcripts encoded on the H strand. This could be explained by different stabilities of the individual mitochondrial transcripts due to up-regulation/down-regulation of factors involved in mitochondrial transcript processing/stability. Previous studies reported that most L-strand transcripts, including *mt-Nd6,* were unaffected when silencing or knocking out the *Lrpprc* gene (*54*, *63*). LRPPRC levels decrease markedly once POLRMT levels drop below 50% of control levels to cause markedly decreased mitochondrial transcription. This finding is consistent with the previously observed reciprocal interdependency between levels of LRPPRC protein and mitochondrial mRNAs (*64*). The strongly increased GRSF1 levels in *Polrmt* knockouts are in line with the less reduced amounts of *mt-Nd6* mRNA in comparison with levels of H-strand transcripts, because GRSF1 has been suggested to be involved in regulating and interacting with *mt-Nd6* mRNA and its precursor strand (*51*, *52*). However, these circumstances cannot explain why tRNAs from the L strand are present at higher levels than tRNAs of the H strand. Hence, a likely explanation for the difference in transcript steady-state levels is the observed promoter-specific transcription initiation effects in heart mitochondria with low POLRMT levels. This is underscored by our in vitro findings that transcription initiation at LSP is better maintained than at HSP at low POLRMT levels. This difference in the strengths of the two promoters is in line with previous in vitro studies (*15*). In conclusion, we found that POLRMT is essential for embryonic development, and that whole-body knockout results in embryonic lethality during midgestation, whereas a moderate reduction of *Polrmt* expression does not cause any phenotype. We further provide the first in vivo evidence that POLRMT functions as the primase for mtDNA replication in mammalian mitochondria. At low POLRMT levels, we observed a significant discrepancy in the initiation of mitochondrial transcription between the HSP and LSP, suggesting that POLRMT is part of a mechanism that provides a switch between RNA primer formation for mtDNA replication and mtDNA expression. Coordinated replication and expression of the mitochondrial genome are essential for metabolically active mammalian cells. By using several mouse models, we characterized the molecular consequences of different expression levels of POLRMT, a key player in those processes and thus a good target for therapeutic strategies.

MATERIALS AND METHODS

Generation and handling of *Polrmt* knockout mice

The targeting vector for disrupting *Polrmt* in embryonic stem cells (derived from C57BL/6N mice) was generated using the bacterial artificial chromosome (BAC) clones from the RPC19-731 BAC library by TaconicArtemis GmbH. To generate knockout *Polrmt* mice exon 3 of the *Polrmt*, locus was flanked by *lox*P sites, and a positive selection marker, PuroR, was flanked by F_3 sites and inserted into intron 2. The puromycin resistance cassette was removed by mating of $Polrmt^{+/loxP\text{-}pur}$ mice with transgenic mice ubiquitously expressing flp recombinase. Resulting $Polrmt^{+/loxP}$ mice were mated with mice ubiquitously expressing cre recombinase to generate heterozygous knockout $Polrmt^{+/-}$ mice (fig. S1). Heart- and skeletal muscle–specific *Polrmt* knockout mice were generated as previously described (*46*). All animal procedures were conducted in accordance with European, national, and institutional guidelines and protocols, and were approved by local government authorities.

DNA isolation, Southern blot analysis, and mtDNA quantification

Total DNA was isolated from heart tissue using the DNeasy Blood & Tissue Kit (Qiagen) and subjected to Southern blot analysis as previously described (*28*). DNA (3 to 10 μg) was digested with Sac I endonuclease, and fragments were separated by agarose gel electrophoresis, transferred to nitrocellulose membranes (Hybond-N^+ membranes; GE Healthcare), and hybridized with [α-^{32}P]dCTP (2′-deoxycytidine 5′-triphosphate)–labeled probes to detect total mtDNA (pAM1), the D loop, or nuclear DNA (18*S* rDNA) as loading control. mtDNA was isolated by phenol/chloroform extraction from purified mitochondria for the detection of the D loop by Southern blotting. Samples were heated for 10 min at 100°C before loading. mtDNA measured by semiquantitative RT-PCR was carried out on 4 ng of total DNA in a 7900HT Real-Time PCR System (Applied Biosystems) using TaqMan probes specific for the *mt-Co1*, *mt-Nd1*, *mt-Nd5*, and *18S* genes (Applied Biosystems).

RT-PCR, qRT-PCR, and Northern blot analysis

RNA was isolated by either using the ToTALLY RNA Isolation Kit (Ambion) or using TRIzol Reagent (Invitrogen) and subjected to DNase treatment (TURBO DNA-free; Ambion). RT-PCR was carried out after cDNA synthesis (High-Capacity cDNA Reverse Transcription Kit; Applied Biosystems). Primers used for the RT-PCR (Fig. 1A) were as follows: Polrmt-E1_forward (a), 5′-CGGCGCTCCGGTGGACCCGAAGCG-3′; Polrmt-E4_forward (b), 5′-GTGGCTTCTGCAGCTCAAGA-3′; Polrmt-E3_reverse (c), 5′-GCATCACGGTGTTGTACATGTGC-3′; Polrmt-E4_reverse (d), 5′-TCTTGAGCTGCAGAAGCCAC-3′; Polrmt-E5_reverse (e), 5′-CGACGAGAAGTGACTGGACCAG-3′; Polrmt-E2_reverse, 5′-TCCAGCAGTTCAGCATGGCC-3′. Real-time qRT-PCR was performed using the TaqMan 2× Universal PCR Master Mix, No AmpErase UNG (Applied Biosystems). The quantity of transcripts was normalized to β_2M as a reference gene transcript. For Northern

blotting, 1 to 2 μg of total RNA were denatured in RNA Sample Loading Buffer (Sigma-Aldrich), separated on 1 or 1.8% formaldehyde-MOPS [3-(N-morpholino) propanesulfonic acid] agarose gels before transfer onto Hybond-N^+ membranes (GE Healthcare) overnight. After ultraviolet (UV) crosslinking, the blots were hybridized with various probes at 65°C in Rapid-hyb buffer (Amersham) and then washed in 2× and 0.2× SSC/0.1% SDS before exposure to film. Mitochondrial probes used for visualization of mt-mRNA and mt-rRNA levels were restriction fragments labeled with [α-^{32}P]dCTP and a random priming kit (Agilent). Different mitochondrial tRNAs and 7*S* RNA were detected using specific oligonucleotides labeled with [γ-^{32}P]ATP. Radioactive signals were detected by autoradiography.

In organello transcription and replication assays

In organello transcription and replication assays were performed on mitochondria isolated from mouse hearts by differential centrifugation as previously described (*28*). In organello transcription assays were carried out as previously reported (*64*). For each in organello replication assay [modified from (*65*)], 1 mg of purified mitochondria was washed in 1 ml of incubation buffer [10 mM tris (pH 7.4), 25 mM sucrose, 75 mM sorbitol, 100 mM KCl, 10 mM K_2HPO_4, 50 μM EDTA, 5 mM $MgCl_2$, 10 mM glutamate, 2.5 mM malate, bovine serum albumin (BSA; 1 mg/ml), and 1 mM adenosine 5′-diphosphate]; resuspended in 500 μl of incubation buffer supplemented with 50 μM dCTP, dTTP (2′-deoxythymidine 5′-triphosphate), dGTP (2′-deoxyguanosine 5′-triphosphate), and 20 μCi of [α-^{32}P]dATP (PerkinElmer); and incubated for 2 hours at 37°C. After incubation, mitochondria were washed three times in 10 mM tris (pH 6.8), 0.15 mM $MgCl_2$, and 10% glycerol. An aliquot of mitochondria was collected for immunoblotting with the VDAC antibody (Millipore) as a loading control. mtDNA was isolated by phenol/chloroform extractions or by Puregene Core Kit A (Qiagen), and radiolabeled replicated DNA was analyzed by D-loop Southern blotting (as described earlier) and visualized by autoradiography. Quantifications of transcript levels were performed using the program MultiGauge with images generated from a PhosphorImager instrument.

RNA sequencing

RNA was isolated from crude heart mitochondria using the miRNeasy Mini Kit (Qiagen), and the concentration, purity, and integrity were confirmed using a Bioanalyzer. RNA-Seq libraries were constructed using the Illumina TruSeq Sample Prep Kit. Paired-end deep sequencing of the mitochondrial RNAs was performed on an Illumina MiSeq according to the manufacturer's instructions. RNA-Seq was performed on mitochondrial RNA from three different control and POLRMT tissue-specific knockout mice aged 3 to 4 weeks. Sequenced reads were aligned to the mouse genome (GRCm38) with HISAT 0.1.6 (*66*) (–fr –rna-strandness RF; total RNA library). Reads that aligned to the mitochondria were extracted and subsequently realigned with spliced alignment disabled to reflect the unspliced nature of the mitochondrial transcriptome and prevent the introduction of spurious splice junctions. Gene-specific counts were summarized with featureCounts 1.3.5-p4 (*67*) (-p -s 2 -Q 10; total RNA library) using the Ensembl 75 gene annotation for nuclear-encoded genes and a modified annotation for mitochondrial genes. The modified annotation contains merged *mt-Atp8*/*mt-Atp6* and *mt-Nd4l*/*mt-Nd4* annotations to reflect their bicistronic nature. Initially, genes with a zero count in any sample were filtered from the count table (in addition to mt-tRNAs), followed by loess and upper quartile normalization for guanine/cytosine content and sequencing depth, performed with EDASeq 2.3.2 (*68*). Differential expression analysis was performed in R 3.2.0 with edgeR 3.11.2 using a generalized linear model approach with tagwise dispersion estimates, and the offsets were generated by EDASeq (*69*).

In vitro transcription assay

Transcription reactions were in 25 μl total volume containing 25 mM tris-HCl (pH 8.0), 10 mM $MgCl_2$, 64 mM NaCl, BSA (100 μg/ml), 1 mM dithiothreitol (DTT), 400 μM ATP, 150 μM guanosine-5′-triphosphate (GTP), 150 μM cytidine-5′-triphosphate (CTP), 10 μM uridine 5′-triphosphate (UTP), 0.02 μM [α-^{32}P]UTP, and 4 U RNase Inhibitor Murine (New England Biolabs). The transcription template was added at 4 nM and consisted of a restriction cut (Hind III/Eco RI), purified (QIAquick PCR Purification Kit) human LSP/HSP plasmid, where a fragment consisting of positions 325 to 742 of human mtDNA was cloned between the Sma I and Hind III sites of pUC18 (*23*). To each reaction, 128 nM human TFB2M and 320 nM human TFAM (corresponding to 1 TFAM per 40 bp) were added. Human POLRMT was added at five different concentrations: 128, 32, 8, 2, and 0.5 nM, respectively. The reactions were incubated at 32°C for 30 min and stopped by the addition of stop buffer [10 mM tris-HCl (pH 8.0), 0.2 M NaCl, 1 mM EDTA, and proteinase K (100 μg/ml)] followed by incubation at 42°C for 45 min. The transcription products were ethanol-precipitated, dissolved in 20 μl loading buffer (98% formamide, 10 mM EDTA, 0.025% xylene cyanol FF, and 0.025% bromophenol blue), and analyzed on 4% denaturing polyacrylamide gels (1× tris-borate EDTA and 7 M urea). Quantifications of transcript levels were performed using the program MultiGauge with images generated from a PhosphorImager instrument.

Western blots, BN-PAGE, antisera, and enzymatic activity

Mitochondria were isolated from mouse heart using differential centrifugation as previously reported (*28*). Proteins were separated by SDS-PAGE (using 4 to 12% bis-tris protein gels; Invitrogen) and then transferred onto polyvinylidene difluoride membranes (GE Healthcare). Immunoblotting was performed according to standard techniques using enhanced chemiluminescence (Immun-Star Horseradish Peroxidase Luminol/Enhancer from Bio-Rad). BN electrophoresis was carried out on 100 μg of mitochondria solubilized with digitonin as previously described (*28*). BN gels were further subjected to immunoblotting or Coomassie Brilliant Blue R staining as indicated. The following antibodies were used: NDUFA9 (complex I) and SDHA (complex II) from Invitrogen; ATP5A1 (complex V), TFAM, MFN2, and POLγA from Abcam; VDAC (porin) and COX1 (complex IV) from MitoSciences; and GRSF1, SSBP1, TEFM, MRPL12, MRPS35, MRPL37, ELAC2, and tubulin from Sigma-Aldrich. Further, polyclonal antisera were used to detect COX2, TFAM, TFB2M, LRPPRC, TWINKLE, LONP, and POLRMT proteins (*25*, *28*, *46*, *54*, *70*). The rabbit polyclonal antisera against recombinant mouse TWINKLE, POLRMT, and TFB2M protein that lack the mitochondrial targeting signal were generated by Agrisera and subsequently affinity-purified using the corresponding recombinant protein. To measure mitochondrial respiratory chain complex activities, 15 to 50 μg of mitochondria were diluted in phosphate buffer [50 mM KH_2PO_4 (pH 7.4)], followed by spectrophotometric analysis of isolated respiratory chain complex activities at 37°C, using a Hitachi UV-3600 spectrophotometer. To follow citrate synthase activity, increase in absorbance at 412 nm was recorded after the addition of 0.1 mM acetyl–coenzyme A, 0.5 mM oxaloacetate, and 0.1 mM 5,5′-dithiobis-2-nitrobenzoic acid. SDH activity was measured

at 600 nm after the addition of 10 mM succinate, 35 μM dichlorphenolindophenol, and 1 mM KCN. NADH dehydrogenase activity was determined at 340 nm after the addition of 0.25 mM NADH, 0.25 mM decylubiquinone, and 1 mM KCN and controlling for rotenone sensitivity. Cytochrome c oxidase activity was measured by standard tetramethyl-*p*-phenylenediamine ascorbate/KCN-sensitive assays. To assess the ATPase activity, frozen isolated mitochondria (65 μg/ml) were incubated at 37°C with 75 mM triethanolamine and 2 mM $MgCl_2$ (pH 8.9). Mitochondria were preincubated for 2 min with alamethicin (10 μg/ml) before addition of 2 mM ATP. Samples were removed every 2 min and precipitated in 7% $HClO_4$ and 25 mM EDTA (50 μl). Phosphate was quantified by incubating an aliquot with 5.34 mM molybdate (1 ml), 28.8 mM ferrous sulfate, and 0.75 N H_2SO_4 for 2 min. The absorbance was assessed at 600 nm. In parallel, oligomycin (2.5 μg per ml protein) was added to the mitochondrial suspension to determine the oligomycin-insensitive ATPase activity. Each activity was normalized to milligram protein by using the Lowry-based Bio-Rad protein detergent-compatible kit. All chemicals were obtained from Sigma-Aldrich.

Linear density glycerol gradients

The mtDNA bound and unbound TFAM pools were assayed using ultracentrifugation through a 10 to 45% linear density glycerol gradient modified from previous studies (*71*). Crude mitochondria (1 to 3 mg) from 4- to 5-week-old mouse hearts were isolated by differential centrifugation as described earlier (*28*), pelleted by centrifugation (15 min, 9300*g*/4°C), and then lysed in buffer containing 5% glycerol, 20 mM NaCl, 30 mM Hepes (pH 8.0), 1 mM EDTA, 2 mM DTT, and 1.2% Triton X-100 supplemented with EDTA-free complete protease inhibitor cocktail and PhosSTOP Tablets (Roche) with 10 strokes in a glass potter on ice. After 10 min of incubation, lysates were cleared by centrifugation (5 min, 800*g*/4°C); overlaid on top of a 10 to 45% linear glycerol gradient prepared in 20 mM NaCl, 25 mM Hepes (pH 8.0), 1 mM EDTA, 1 mM DTT, 0.2% Triton X-100, and EDTA-free complete protease inhibitor cocktail (Roche); and centrifuged in an SW 41 rotor at 210,000*g*/4°C for 3 hours in a Beckman Coulter Optima L-100 XP ultracentrifuge. Gradients were prepared using Gradient Master (Biocomp Instruments Inc) in 14 mm × 89 mm Ultra-Clear Centrifuge Tubes (Beckman Instruments Inc.). Fractions (750 μl) were collected from the top of the gradients, and 20 μl of each fraction was analyzed by SDS-PAGE (Invitrogen) and Western blotting. For analysis of mtDNA sedimentation profiles, mtDNA was isolated from two-thirds of each fraction using phenol/chloroform extraction digested with Sac I and subjected to Southern blotting.

Morphological analysis (heart sections)

Hematoxylin and eosin stainings were performed on paraformaldehyde (PFA)–fixed cryosections from 4-week-old mouse hearts that were immediately embedded in OCT Tissue-Tek in cooled methyl-butan. Images of heart sections were generated by stitching of several images taken with the Nikon Eclipse Ci microscope. For transmission electron microscopy, pieces of the mouse heart apex were fixed in 2% glutaraldehyde and 2% PFA in 0.1 M sodium cacodylate buffer (pH 7.4). Specimens were postfixed in 1% osmium tetroxide [in 0.1 M sodium cacodylate buffer (pH 7.4)]. After thorough washing with water, specimens were dehydrated in ethanol followed by acetone and embedded in medium-grade Agar Low Viscosity Resin (Plano). Ultrathin sections (70 to 80 nm) were cut with a Reichert-Jung Ultracut E Ultramicrotome, stained with 2% uranyl acetate in 70% ethanol, followed by lead citrate, and examined with a Hitachi H-7650 transmission electron microscope operating at 100 kV fitted with a midmounted AMT XR41-M digital camera (Advanced Microscopy Techniques).

Statistical analysis

Experiments were performed at least in triplicates, and results are representative of $n = 3$ independent biological experiments. All values are expressed as means ± SEM, unless indicated differently. Statistical significance was assessed by using two-tailed unpaired Student's *t* test. Differences were considered statistically significant at a value of $P < 0.05$ ($^{*}P < 0.05$, $^{**}P < 0.01$, and $^{***}P < 0.001$).

SUPPLEMENTARY MATERIALS

Supplementary material for this article is available at http://advances.sciencemag.org/cgi/content/full/2/8/e1600963/DC1

fig. S1. Targeting strategy for disrupting the *Polrmt* gene in mouse.
fig. S2. ECG analysis of conditional *Polrmt* knockout mice.
fig. S3. Total protein levels of nuclear-encoded factors involved in mtDNA expression.
fig. S4. Steady-state mitochondrial protein levels of conditional *Polrmt* knockout mice.
fig. S5. Relative mitochondrial protein distribution across a gradient.
fig. S6. Relative mitochondrial protein distribution in *Polrmt* knockout mice.
fig. S7. Respiratory chain complex protein levels in heterozygous *Polrmt* knockout mice.
fig. S8. Relative mitochondrial RNA abundance in heterozygous *Polrmt* knockout mice.
fig. S9. Steady-state mitochondrial protein levels in heterozygous *Polrmt* knockout hearts.
fig. S10. mtDNA levels in heterozygous *Polrmt* knockout hearts.
table S1. Summary statistics and *P* values of RT-qPCR presented in Fig. 4B.

REFERENCES AND NOTES

1. D. M. Turnbull, P. Rustin, Genetic and biochemical intricacy shapes mitochondrial cytopathies. *Neurobiol. Dis.* **92** (pt. A), 55–63 (2015).
2. N.-G. Larsson, Somatic mitochondrial DNA mutations in mammalian aging. *Annu. Rev. Biochem.* **79**, 683–706 (2010).
3. C. M. Gustafsson, M. Falkenberg, N.-G. Larsson, Maintenance and expression of mammalian mitochondrial DNA. *Annu. Rev. Biochem.* **85**, 133–160 (2016).
4. M. Gaspari, M. Falkenberg, N.-G. Larsson, C. M. Gustafsson, The mitochondrial RNA polymerase contributes critically to promoter specificity in mammalian cells. *EMBO J.* **23**, 4606–4614 (2004).
5. B. M. Hallberg, N.-G. Larsson, Making proteins in the powerhouse. *Cell Metab.* **20**, 226–240 (2014).
6. S. Crews, D. Ojala, J. Posakony, J. Nishiguchi, G. Attardi, Nucleotide sequence of a region of human mitochondrial DNA containing the precisely identified origin of replication. *Nature* **277**, 192–198 (1979).
7. D. D. Chang, D. A. Clayton, Precise identification of individual promoters for transcription of each strand of human mitochondrial DNA. *Cell* **36**, 635–643 (1984).
8. J. Montoya, T. Christianson, D. Levens, M. Rabinowitz, G. Attardi, Identification of initiation sites for heavy-strand and light-strand transcription in human mitochondrial DNA. *Proc. Natl. Acad. Sci. U.S.A.* **79**, 7195–7199 (1982).
9. D. Ojala, J. Montoya, G. Attardi, tRNA punctuation model of RNA processing in human mitochondria. *Nature* **290**, 470–474 (1981).
10. B. S. Masters, L. L. Stohl, D. A. Clayton, Yeast mitochondrial RNA polymerase is homologous to those encoded by bacteriophages T3 and T7. *Cell* **51**, 89–99 (1987).
11. R. Ringel, M. Sologub, Y. I. Morozov, D. Litonin, P. Cramer, D. Temiakov, Structure of human mitochondrial RNA polymerase. *Nature* **478**, 269–273 (2011).
12. M. Falkenberg, M. Gaspari, A. Rantanen, A. Trifunovic, N.-G. Larsson, C. M. Gustafsson, Mitochondrial transcription factors B1 and B2 activate transcription of human mtDNA. *Nat. Genet.* **31**, 289–294 (2002).
13. M. Sologub, D. Litonin, M. Anikin, A. Mustaev, D. Temiakov, TFB2 is a transient component of the catalytic site of the human mitochondrial RNA polymerase. *Cell* **139**, 934–944 (2009).
14. K. Schwinghammer, A. C. M. C., Y. I. Morozov, K. Agaronyan, D. Temiakov, P. Cramer, Structure of human mitochondrial RNA polymerase elongation complex. *Nat. Struct. Mol. Biol.* **20**, 1298–1303 (2013).
15. Y. Shi, A. Dierckx, P. H. Wanrooij, S. Wanrooij, N.-G. Larsson, L. Marcus Wilhelmsson, M. Falkenberg, C. M. Gustafsson, Mammalian transcription factor A is a core component of the mitochondrial transcription machinery. *Proc. Natl. Acad. Sci. U.S.A.* **109**, 16510–16515 (2012).

16. R. P. Fisher, J. N. Topper, D. A. Clayton, Promoter selection in human mitochondria involves binding of a transcription factor to orientation-independent upstream regulatory elements. *Cell* **50**, 247–258 (1987).
17. D. J. Dairaghi, G. S. Shadel, D. A. Clayton, Human mitochondrial transcription factor A and promoter spacing integrity are required for transcription initiation. *Biochim. Biophys. Acta* **1271**, 127–134 (1995).
18. V. Posse, E. Hoberg, A. Dierckx, S. Shahzad, C. Koolmeister, N.-G. Larsson, L. Marcus Wilhelmsson, B. Martin Hällberg, C. M. Gustafsson, The amino terminal extension of mammalian mitochondrial RNA polymerase ensures promoter specific transcription initiation. *Nucleic Acids Res.* **42**, 3638–3647 (2014).
19. Y. I. Morozov, A. V. Parshin, K. Agaronyan, A. C. M. Cheung, M. Anikin, P. Cramer, D. Temiakov, A model for transcription initiation in human mitochondria. *Nucleic Acids Res.* **43**, 3726–3735 (2015).
20. D. F. Bogenhagen, D. Rousseau, S. Burke, The layered structure of human mitochondrial DNA nucleoids. *J. Biol. Chem.* **283**, 3665–3675 (2008).
21. C. Kukat, K. M. Davies, C. A. Wurm, H. Spåhr, N. A. Bonekamp, I. Kühl, F. Joos, P. Loguercio Polosa, C. Bae Park, V. Posse, M. Falkenberg, S. Jakobs, W. Kühlbrandt, N.-G. Larsson, Cross-strand binding of TFAM to a single mtDNA molecule forms the mitochondrial nucleoid. *Proc. Natl. Acad. Sci. U.S.A.* **112**, 11288–11293 (2015).
22. M. I. Ekstrand, M. Falkenberg, A. Rantanen, C. Bae Park, M. Gaspari, K. Hultenby, P. Rustin, C. M. Gustafsson, N.-G. Larsson, Mitochondrial transcription factor A regulates mtDNA copy number in mammals. *Hum. Mol. Genet.* **13**, 935–944 (2004).
23. G. Farge, M. Mehmedovic, M. Baclayon, S. M. J. L. van den Wildenberg, W. H. Roos, C. M. Gustafsson, G. J. L. Wuite, M. Falkenberg, In vitro-reconstituted nucleoids can block mitochondrial DNA replication and transcription. *Cell Rep.* **8**, 66–74 (2014).
24. Y. Matsushima, Y.-i. Goto, L. S. Kaguni, Mitochondrial Lon protease regulates mitochondrial DNA copy number and transcription by selective degradation of mitochondrial transcription factor A (TFAM). *Proc. Natl. Acad. Sci. U.S.A.* **107**, 18410–18415 (2010).
25. B. Lu, J. Lee, X. Nie, M. Li, Y. I. Morozov, S. Venkatesh, D. F. Bogenhagen, D. Temiakov, C. K. Suzuki, Phosphorylation of human TFAM in mitochondria impairs DNA binding and promotes degradation by the AAA+ Lon protease. *Mol. Cell* **49**, 121–132 (2013).
26. N. Hance, M. I. Ekstrand, A. Trifunovic, Mitochondrial DNA polymerase gamma is essential for mammalian embryogenesis. *Hum. Mol. Genet.* **14**, 1775–1783 (2005).
27. M. M. Humble, M. J. Young, J. F. Foley, A. R. Pandiri, G. S. Travlos, W. C. Copeland, *Polg2* is essential for mammalian embryogenesis and is required for mtDNA maintenance. *Hum. Mol. Genet.* **22**, 1017–1025 (2013).
28. D. Milenkovic, S. Matic, I. Kühl, B. Ruzzenente, C. Freyer, E. Jemt, C. Bae Park, M. Falkenberg, N.-G. Larsson, TWINKLE is an essential mitochondrial helicase required for synthesis of nascent D-loop strands and complete mtDNA replication. *Hum. Mol. Genet.* **22**, 1983–1993 (2013).
29. P. Cantatore, G. Attardi, Mapping of nascent light and heavy strand transcripts on the physical map of HeLa cell mitochondrial DNA. *Nucleic Acids Res.* **8**, 2605–2625 (1980).
30. D. D. Chang, W. W. Hauswirth, D. A. Clayton, Replication priming and transcription initiate from precisely the same site in mouse mitochondrial DNA. *EMBO J.* **4**, 1559–1567 (1985).
31. D. D. Chang, D. A. Clayton, Priming of human mitochondrial DNA replication occurs at the light-strand promoter. *Proc. Natl. Acad. Sci. U.S.A.* **82**, 351–355 (1985).
32. X. H. Pham, G. Farge, Y. Shi, M. Gaspari, C. M. Gustafsson, M. Falkenberg, Conserved sequence box II directs transcription termination and primer formation in mitochondria. *J. Biol. Chem.* **281**, 24647–24652 (2006).
33. B. Xu, D. A. Clayton, A persistent RNA-DNA hybrid is formed during transcription at a phylogenetically conserved mitochondrial DNA sequence. *Mol. Cell Biol.* **15**, 580–589 (1995).
34. J. P. Uhler, M. Falkenberg, Primer removal during mammalian mitochondrial DNA replication. *DNA Repair* **34**, 28–38 (2015).
35. S. García-Gómez, A. Reyes, M. I. Martínez-Jiménez, E. S. Chocrón, S. Mourón, G. Terrados, C. Powell, E. Salido, J. Méndez, I. J. Holt, L. Blanco, PrimPol, an archaic primase/polymerase operating in human cells. *Mol. Cell* **52**, 541–553 (2013).
36. M. Falkenberg, N.-G. Larsson, C. M. Gustafsson, DNA replication and transcription in mammalian mitochondria. *Annu. Rev. Biochem.* **76**, 679–699 (2007).
37. I. J. Holt, A. Reyes, Human mitochondrial DNA replication. *Cold Spring Harb. Perspect. Biol.* **4**, a012971 (2012).
38. D. A. Clayton, Replication of animal mitochondrial DNA. *Cell* **28**, 693–705 (1982).
39. J. M. Fusté, S. Wanrooij, E. Jemt, C. E. Granycome, T. J. Cluett, Y. Shi, N. Atanassova, I. J. Holt, C. M. Gustafsson, M. Falkenberg, Mitochondrial RNA polymerase is needed for activation of the origin of light-strand DNA replication. *Mol. Cell* **37**, 67–78 (2010).
40. S. Wanrooij, J. Miralles Fusté, G. Farge, Y. Shi, C. M. Gustafsson, M. Falkenberg, Human mitochondrial RNA polymerase primes lagging-strand DNA synthesis in vitro. *Proc. Natl. Acad. Sci. U.S.A.* **105**, 11122–11127 (2008).
41. D. Bogenhagen, D. A. Clayton, Mechanism of mitochondrial DNA replication in mouse L-cells: Kinetics of synthesis and turnover of the initiation sequence. *J. Mol. Biol.* **119**, 49–68 (1978).
42. M. Minczuk, J. He, A. M. Duch, T. J. Ettema, A. Chlebowski, K. Dzionek, L. G. J. Nijtmans, M. A. Huynen, I. J. Holt, TEFM (c17orf42) is necessary for transcription of human mtDNA. *Nucleic Acids Res.* **39**, 4284–4299 (2011).
43. V. Posse, S. Shahzad, M. Falkenberg, B. M. Hällberg, C. M. Gustafsson, TEFM is a potent stimulator of mitochondrial transcription elongation in vitro. *Nucleic Acids Res.* **43**, 2615–2624 (2015).
44. K. Agaronyan, Y. I. Morozov, M. Anikin, D. Temiakov, Replication-transcription switch in human mitochondria. *Science* **347**, 548–551 (2015).
45. N. G. Larsson, J. Wang, H. Wilhelmsson, A. Oldfors, P. Rustin, M. Lewandoski, G. S. Barsh, D. A. Clayton, Mitochondrial transcription factor A is necessary for mtDNA maintenance and embryogenesis in mice. *Nat. Genet.* **18**, 231–236 (1998).
46. I. Kühl, C. Kukat, B. Ruzzenente, D. Milenkovic, A. Mourier, M. Miranda, C. Koolmeister, M. Falkenberg, N.-G. Larsson, POLRMT does not transcribe nuclear genes. *Nature* **514**, E7–E11 (2014).
47. A. M. Gillum, D. A. Clayton, Mechanism of mitochondrial DNA replication in mouse L-cells: RNA priming during the initiation of heavy-strand synthesis. *J. Mol. Biol.* **135**, 353–368 (1979).
48. D. Litonin, M. Sologub, Y. Shi, M. Savkina, M. Anikin, M. Falkenberg, C. M. Gustafsson, D. Temiakov, Human mitochondrial transcription revisited: Only TFAM and TFB2M are required for transcription of the mitochondrial genes in vitro. *J. Biol. Chem.* **285**, 18129–18133 (2010).
49. L. K. Brzezniak, M. Bijata, R. J. Szczesny, P. P. Stepien, Involvement of human ELAC2 gene product in 3′ end processing of mitochondrial tRNAs. *RNA Biol.* **8**, 616–626 (2011).
50. M. I. G. Lopez Sanchez, T. R. Mercer, S. M. K. Davies, A.-M. J. Shearwood, K. K. A. Nygård, T. R. Richman, J. S. Mattick, O. Rackham, A. Filipovska, RNA processing in human mitochondria. *Cell Cycle* **10**, 2904–2916 (2011).
51. A. A. Jourdain, M. Koppen, M. Wydro, C. D. Rodley, R. N. Lightowlers, Z. M. Chrzanowska-Lightowlers, J.-C. Martinou, GRSF1 regulates RNA processing in mitochondrial RNA granules. *Cell Metab.* **17**, 399–410 (2013).
52. H. Antonicka, F. Sasarman, T. Nishimura, V. Paupe, E. A. Shoubridge, The mitochondrial RNA-binding protein GRSF1 localizes to RNA granules and is required for post-transcriptional mitochondrial gene expression. *Cell Metab.* **17**, 386–398 (2013).
53. F. Sasarman, C. Brunel-Guitton, H. Antonicka, T. Wai, E. A. Shoubridge; LSFC Consortium, LRPPRC and SLIRP interact in a ribonucleoprotein complex that regulates post-transcriptional gene expression in mitochondria. *Mol. Biol. Cell* **21**, 1315–1323 (2010).
54. B. Ruzzenente, M. D. Metodiev, A. Wredenberg, A. Bratic, C. B. Park, Y. Cámara, D. Milenkovic, V. Zickermann, R. Wibom, K. Hultenby, H. Erdjument-Bromage, P. Tempst, U. Brandt, J. B. Stewart, C. M. Gustafsson, N. G. Larsson, LRPPRC is necessary for polyadenylation and coordination of translation of mitochondrial mRNAs. *EMBO J.* **31**, 443–456 (2012).
55. Y. V. Surovtseva, T. E. Shutt, J. Cotley, H. Cimen, S. Y. Chen, E. C. Koc, G. S. Shadel, Mitochondrial ribosomal protein L12 selectively associates with human mitochondrial RNA polymerase to activate transcription. *Proc. Natl. Acad. Sci. U.S.A.* **108**, 17921–17926 (2011).
56. N. G. Larsson, A. Oldfors, E. Holme, D. A. Clayton, Low levels of mitochondrial transcription factor A in mitochondrial DNA depletion. *Biochem. Biophys. Res. Commun.* **200**, 1374–1381 (1994).
57. C. Kukat, C. A. Wurm, H. Spåhr, M. Falkenberg, N.-G. Larsson, S. Jakobs, Super-resolution microscopy reveals that mammalian mitochondrial nucleoids have a uniform size and frequently contain a single copy of mtDNA. *Proc. Natl. Acad. Sci. U.S.A.* **180**, 13534–13539 (2011).
58. E. Jemt, Ö. Persson, Y. Shi, M. Mehmedovic, J. P. Uhler, M. Dávila López, C. Freyer, C. M. Gustafsson, T. Samuelsson, M. Falkenberg, Regulation of DNA replication at the end of the mitochondrial D-loop involves the helicase TWINKLE and a conserved sequence element. *Nucleic Acids Res.* **43**, 9262–9275 (2015).
59. P. L. Polosa, S. Deceglie, M. Roberti, M. N. Gadaleta, P. Cantatore, Contrahelicase activity of the mitochondrial transcription termination factor mtDBP. *Nucleic Acids Res.* **33**, 3812–3820 (2005).
60. A. Picca, A. M. S. Lezza, Regulation of mitochondrial biogenesis through TFAM-mitochondrial DNA interactions: Useful insights from aging and calorie restriction studies. *Mitochondrion* **25**, 67–75 (2015).
61. A. Hansson, N. Hance, E. Dufour, A. Rantanen, K. Hultenby, D. A. Clayton, R. Wibom, N.-G. Larsson, A switch in metabolism precedes increased mitochondrial biogenesis in respiratory chain-deficient mouse hearts. *Proc. Natl. Acad. Sci. U.S.A.* **101**, 3136–3141 (2004).
62. A. Reyes, L. Kazak, S. R. Wood, T. Yasukawa, H. T. Jacobs, I. J. Holt, Mitochondrial DNA replication proceeds via a 'bootlace' mechanism involving the incorporation of processed transcripts. *Nucleic Acids Res.* **41**, 5837–5850 (2013).
63. A. R. Wolf, V. K. Mootha, Functional genomic analysis of human mitochondrial RNA processing. *Cell Rep.* **7**, 918–931 (2014).
64. M. Lagouge, A. Mourier, H. J. Lee, H. Spåhr, T. Wai, C. Kukat, E. S. Ramos, E. Motori, J. D. Busch, S. Siira; German Mouse Clinic Consortium, E. Kremmer, A. Filipovska, N.-G. Larsson, SLIRP regulates the rate of mitochondrial protein synthesis and protects LRPPRC from degradation. *PLOS Genet.* **11**, e1005423 (2015).
65. S. Gensler, K. Weber, W. E. Schmitt, A. Pérez-martos, J. A. Enriquez, J. Montoya, R. J. Wiesner, Mechanism of mammalian mitochondrial DNA replication: Import of mitochondrial transcription factor A into isolated mitochondria stimulates 7S DNA synthesis. *Nucleic Acids Res.* **29**, 3657–3663 (2001).

66. D. Kim, B. Langmead, S. L. Salzberg, HISAT: A fast spliced aligner with low memory requirements. *Nat. Methods* **12**, 357–360 (2015).
67. Y. Liao, G. K. Smyth, W. Shi, featureCounts: An efficient general purpose program for assigning sequence reads to genomic features. *Bioinformatics* **30**, 923–930 (2014).
68. D. Risso, K. Schwartz, G. Sherlock, S. Dudoit, GC-content normalization for RNA-seq data. *BMC Bioinformatics* **12**, 480 (2011).
69. M. D. Robinson, D. J. McCarthy, G. K. Smyth, edgeR: A bioconductor package for differential expression analysis of digital gene expression data. *Bioinformatics* **26**, 139–140 (2010).
70. J. Harmel, B. Ruzzenente, M. Terzioglu, H. Spåhr, M. Falkenberg, N.-G. Larsson, The leucine-rich pentatricopeptide repeat-containing protein (LRPPRC) does not activate transcription in mammalian mitochondria. *J. Biol. Chem.* **288**, 15510–15519 (2013).
71. K.-W. Lee, C. Okot-Kotber, J. F. LaComb, D. F. Bogenhagen, Mitochondrial ribosomal RNA (rRNA) methyltransferase family members are positioned to modify nascent rRNA in foci near the mitochondrial DNA nucleoid. *J. Biol. Chem.* **288**, 31386–31399 (2013).
72. Y. Cámara, J. Asin-Cayuela, C. B. Park, M. D. Metodiev, Y. Shi, B. Ruzzenente, C. Kukat, B. Habermann, R. Wibom, K. Hultenby, T. Franz, H. Erdjument-Nromage, P. Tempst, B. M. Hallberg, C. M. Gustafsson, N.-G. Larsson, MTERF4 regulates translation by targeting the methyltransferase NSUN4 to the mammalian mitochondrial ribosome. *Cell Metab.* **13**, 527–539 (2011).

Acknowledgments: We thank N. Hochhard for technical assistance and C. K. Suzuki for providing the mouse LONP antibody. RNA library construction and sequencing were performed at the Cologne Center for Genomics. ECG analysis was performed with the ECG screening system of the phenotyping core facility, Max Planck Institute for Biology of Ageing. We are grateful for the technical support from the CECAD Imaging Facility and the FACS & Imaging Core Facility of the Max Planck Institute for Biology of Ageing. **Funding:** This study was supported by a European Research Council Advanced Investigator grant (268897), the Swedish Research Council (2015-0418 2013-2859), and the Knut and Alice Wallenberg Foundation to N.-G.L. C.M.G. was funded by the Swedish Research Council (2012-2583), the Swedish Cancer Foundation, and the Knut and Alice Wallenberg Foundation. A.F. is a National Health and Medical Research Council Senior Research Fellow (APP 1058442), supported by an Alexander von Humboldt Fellowship for experienced researchers and by the National Health and Medical Research Council (APP1078273). **Author contributions:** Conceived and designed the experiments: I.K., P.L.P., C.M.G., and N.-G.L. Performed experiments: I.K., M.M., V.P., D.M., A.M., N.A.B., U.N., P.L.P., and A.F. Analyzed the data: I.K., M.M., V.P., S.J.S., and A.F. Wrote the paper: I.K., C.M.G., and N.-G.L. **Competing interests:** The authors declare that they have no competing interests. **Data and materials availability:** RNA-Seq data have been deposited in the Gene Expression Omnibus repository under accession no. GSE83368. Additional data related to this paper may be requested from the authors. Knockout mouse models presented in the paper must be obtained through a material transfer agreement.

Submitted 2 May 2016
Accepted 1 July 2016
Published 5 August 2016
10.1126/sciadv.1600963

Citation: I. Kühl, M. Miranda, V. Posse, D. Milenkovic, A. Mourier, S. J. Siira, N. A. Bonekamp, U. Neumann, A. Filipovska, P. L. Polosa, C. M. Gustafsson, N.-G. Larsson, POLRMT regulates the switch between replication primer formation and gene expression of mammalian mtDNA. *Sci. Adv.* **2**, e1600963 (2016).